01 Jan 1998

A Maximum Torque Per Ampere Control Strategy for Induction Motor Drives

O. Wasynczuk

Keith Corzine
Missouri University of Science and Technology

S. D. Sudhoff

Jerry L. Tichenor

et. al. For a complete list of authors, see https://scholarsmine.mst.edu/ele_comeng_facwork/723

A Maximum Torque per Ampere Control Strategy for Induction Motor Drives

O. Wasynczuk, S. D. Sudhoff,
K. A. Corzine, Jerry L. Tichenor, P. C. Krause
P. C. Krause and Associates, Inc.
West Lafayette, Indiana 47906

I. G. Hansen, L. M. Taylor
NASA Lewis Research Center
Cleveland, Ohio, 44135

Abstract - In this paper, a new control strategy is proposed which is simple in structure and has the straightforward goal of minimizing the stator current amplitude for a given load torque. It is shown that the resulting induction motor efficiency is reasonably close to optimal and that the approach is insensitive to variations in rotor resistance. Although the torque response is not as fast as in field-oriented control strategies, the response is reasonably fast. In fact, if the mechanical time constant is large relative to the rotor time constant, which is frequently the case, the sacrifice in dynamic performance is insignificant relative to FO strategies.

I. INTRODUCTION

Field-oriented (FO) induction motor drive systems provide an ability to rapidly and accurately control the electromagnetic torque [1-2]. A disadvantage is that in order to maintain a fast speed-of-response, it is necessary to operate at rated flux even at low values of torque. Thus, the efficiency and power factor can be quite poor at low torques, regardless of rotor speed. Additionally, accurate knowledge of the rotor resistance is necessary requiring on-line sensing and adaption approaches [2].

An extensive amount of research has also been conducted in the areas of optimum efficiency control of induction motor drive systems [3-8]. It has long been recognized that for a given torque and speed, it is possible to adjust the slip frequency so as to minimize resistive and core losses thus maximizing the efficiency of the induction motor. Due to the complexity of the loss models, optimization was either performed numerically with the calculated optimum slip stored in a look-up table [3-5] or using on-line search techniques [6-8]. A disadvantage of the table-look-up approach is the necessity of accurate machine parameters which vary from one machine to another. Disadvantages of on-line search approaches include their complexity and their potential to exhibit hunting.

In this paper, a new control strategy is proposed which is simple in structure and has the straightforward goal of minimizing the stator current amplitude for a given load torque. It is shown that the resulting induction motor efficiency is reasonably

close to optimal and that the approach is insensitive to variations in rotor resistance. Although the torque response is not as fast as in FO control strategies, the response is reasonably fast making the proposed controller well suited to applications where both dynamic response and high efficiency are important.

II. BACKGROUND

The dynamic equations of the induction machine can be expressed in the synchronous reference frame as [9]

$$v_{qs}^e = r_s i_{qs}^e + p\psi_{qs}^e + \frac{\omega_e}{\omega_b}\psi_{ds}^e \tag{1}$$

$$v_{ds}^e = r_s i_{ds}^e + p\psi_{ds}^e - \frac{\omega_e}{\omega_b}\psi_{qs}^e \tag{2}$$

$$v_{qr}^e = r_r i_{qr}^e + \frac{1}{\omega_b}p\psi_{qr}^e + \frac{(\omega_e - \omega_r)}{\omega_b}\psi_{dr}^e \tag{3}$$

$$v_{dr}^e = r_r i_{dr}^e + \frac{1}{\omega_b}p\psi_{dr}^e - \frac{(\omega_e - \omega_r)}{\omega_b}\psi_{qr}^e \tag{4}$$

$$\psi_{qs}^e = X_{ss}i_{qs}^e + X_M i_{qr}^e ; \quad \psi_{ds}^e = X_{ss}i_{ds}^e + X_M i_{dr}^e \tag{5}$$

$$\psi_{qr}^e = X_{rr}i_{qr}^e + X_M i_{qs}^e ; \quad \psi_{dr}^e = X_{ss}i_{dr}^e + X_M i_{ds}^e \tag{6}$$

It is assumed that all rotor variables are referred to the stator. With stator currents as inputs and rotor windings short circuited, the state equations may be expressed

$$0 = \frac{r_r}{X_{rr}}(\psi_{qr}^e - X_M i_{qs}^e) + \frac{\omega_s}{\omega_b}\psi_{dr}^e + \frac{1}{\omega_b}p\psi_{qr}^e \tag{7}$$

$$0 = \frac{r_r}{X_{rr}}(\psi_{dr}^e - X_M i_{ds}^e) - \frac{\omega_s}{\omega_b}\psi_{qr}^e + \frac{1}{\omega_b}p\psi_{dr}^e \tag{8}$$

where $\omega_s = \omega_e - \omega_r$ is the slip frequency. The stator flux linkages may be expressed in terms of the state variables as

$$\psi_{qs}^e = X'' i_{qs}^e + \frac{X_M}{X_{rr}}\psi_{qr}^e ; \quad \psi_{ds}^e = X'' i_{ds}^e + \frac{X_M}{X_{rr}}\psi_{dr}^e \tag{9}$$

where

$$X'' = X_{ls} + \frac{X_m X_{lr}}{X_m + X_{lr}} \tag{10}$$

is the subtransient reactance. The electromagnetic torque can be expressed,

$$T_e = K(\psi_{dr}^e i_{qs}^e - \psi_{qr}^e i_{ds}^e) \tag{11}$$

If the variables are expressed in SI units, $K = \frac{3}{2}\frac{P}{2}\frac{1}{\omega_b}$. If the variables are expressed in per unit, $K = 1$. In the indirect

method of (FO) control [1], $\theta_e(0)$ is selected such that ψ^e_{qr} is identically zero [1]. Thus, (7) and (8) become

$$0 = -\frac{r_r X_M}{X_{rr}} i^e_{qs} + \frac{\omega_s}{\omega_b} \psi^e_{dr} \tag{12}$$

$$0 = \frac{r_r}{X_{rr}}(\psi^e_{dr} - X_M i^e_{ds}) + \frac{1}{\omega_b} p\psi^e_{dr} \tag{13}$$

If i^e_{ds} is controlled so that it remains constant, (13) implies that $p\psi^e_{dr} = 0$ and

$$\psi^e_{dr} = X_M i^e_{ds} \tag{14}$$

Substituting into (12) and solving for ω_s

$$\omega_s = \frac{\omega_b r_r i^e_{qs}}{X_{rr} i^e_{ds}} \tag{15}$$

The electromagnetic torque (11) can be expressed

$$T_e = K \frac{X^2_M}{X_{rr}} i^e_{qs} i^e_{ds} \tag{16}$$

A block diagram of the (FO) controller is shown in Fig. 1. Therein, i^{e*}_{ds} is the commanded magnetization current which is normally constant and i^{e*}_{qs} is used to control the torque. The current command signals i^*_{as}, i^*_{bs}, and i^*_{cs} are supplied to the inverter control system.
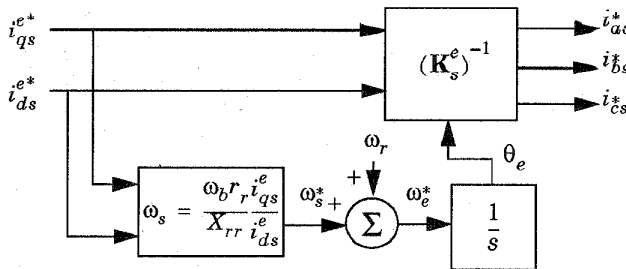

Fig. 1 Block diagram of indirect method field-oriented controller.

III. DEFINITION OF ALTERNATIVE OPERATING STRATEGIES

The following definitions are useful in subsequent analyses. The stator current amplitude is defined as the peak ac current. In terms of qd variables,

$$|i_s| = \sqrt{(i^e_{qs})^2 + (i^e_{ds})^2} \tag{17}$$

The stator flux amplitude is similarly defined as

$$|\psi_s| = \sqrt{(\psi^e_{qs})^2 + (\psi^e_{ds})^2} \tag{18}$$

The efficiency is defined as the output power divided by the electric power supplied to the stator (converter losses are not included). In per unit,

$$\eta = \frac{T_e(\omega_r/\omega_b)}{P_e} \tag{19}$$

where

$$P_e = v^e_{qs} i^e_{qs} + v^e_{ds} i^e_{ds} \tag{20}$$

The conventional power factor is defined as the input power divided by the apparent power.

$$pf = P_e/(\sqrt{P^2_e + Q^2_e}) \tag{21}$$

where

$$Q_e = v^e_{qs} i^e_{ds} - v^e_{ds} i^e_{qs} \tag{22}$$

In the following analysis, it is convenient to select T_e, ω_r, and ω_s as independent variables. All other variables such as stator or rotor flux amplitude, efficiency, or power factor, can be expressed in terms of the selected independent variables. When defining the alternative operating strategies, it is assumed that the torque and speed are given whereupon the slip frequency is adjusted so as to achieve certain characteristics such as maximization of power factor, minimization of stator current, maximization of efficiency, etc.

It must be emphasized that the model presented in Section II does not include the stator or rotor core (hysteresis and eddy current) losses. This does not mean that these losses are negligible; however, it is convenient to postpone consideration of these losses until a later section.

Maximum torque per stator ampere

Operation at maximum torque per ampere is achieved when, at a given torque and speed, the slip frequency is adjusted so that the stator current amplitude is minimized. This mode of operation is subsequently referred to as the maximum torque per ampere (MTA) strategy. An expression for the slip frequency which minimizes the stator current amplitude is easily established by noting that to maximize the product of i^e_{qs} and i^e_{ds} subject to the constraint that (17) is constant, i^e_{qs} should be set equal to i^e_{ds}. Thus from (15),

$$\omega_{s,\text{MTA}} = \frac{\omega_b r_r}{X_{rr}} = \frac{1}{\tau_r} \tag{23}$$

where τ_r is the rotor time constant. This suggests that to maintain minimum stator current, the induction machine should operate at a constant slip equal to the inverse rotor time constant.

Maximum efficiency

In this mode of operation, the slip frequency is adjusted so that the efficiency (19) is maximized. An expression for the slip which maximizes efficiency may be derived by substituting (16) and (20) into (19), and expressing all variables in terms of slip frequency. After considerable algebraic manipulation

$$\eta = \frac{X^2_m r_r \omega_r \omega_s}{r^2_r r_r \omega^2_b + X^2_m r_r \omega^2_s + X^2_{rr} r_s \omega^2_s + X^2_m r_r \omega_r \omega_s} \tag{24}$$

Differentiating with respect to ω_s, setting the resulting expression to zero, and solving for ω_s yields

$$\omega_{s,\text{ME}} = \sqrt{\frac{r^2_r r_s \omega^2_b}{r_r X^2_m + r_s X^2_{rr}}} \tag{25}$$

To maintain maximum efficiency (ME) the machine should operate at a constant slip equal to that calculated in (25). It is interesting to note that the efficiency is independent of torque and the maximizing slip is independent of the torque or speed. The previ-

ous expression for efficiency is optimistic since it does not include the effect of core losses. Also, the optimizing slip may differ somewhat from the value calculated using (25).

Maximum power factor

In this mode of operation, the slip frequency is adjusted so as to maximize the power factor (20). An expression for the slip frequency which maximizes power factor may be derived by substituting (19) and (21) into (20), expressing all variables in terms of slip frequency, differentiating with respect to ω_s, setting the resulting expression to zero, and solving for ω_s. Although this is possible, the resulting expression is too lengthy to be of practical value. Alternatively, the maximization of power factor can be achieved by developing a numerical procedure or function which calculates the power factor as a function of the selected independent variables and, for a given torque and speed, calculating the maximizing slip using well-established algorithms. It can be shown that the power factor and the slip frequency at maximum power factor (MPF) are independent of torque.

Field Oriented Control

In this mode of operation, the d-axis current is set to a constant value which yields rated torque at rated stator flux. The corresponding slip is calculated in accordance with (15). The value of the d-axis current which yields rated torque at rated stator flux may be calculated by substituting the flux linkages in (9) into (18) and expressing all variables in terms of i_{ds}^e. After extensive manipulation,

$$i_{ds}^e = \sqrt{\frac{1}{2a} + \frac{1}{2a}\sqrt{1 - 4a(X'')^2 X_{rr}^2 / X_m^4}} \tag{26}$$

where

$$a = \left[(X'')^2 + \frac{X_m^4}{X_{rr}^2} + \frac{2X_m^2 X''}{X_{rr}} \right] \tag{27}$$

IV. OPERATING CONSTRAINTS

Operation at maximum efficiency, maximum power factor, or minimum stator current may not be achievable for the entire speed and torque range due to operating constraints. Herein, it is assumed that three constraints exist: (1) the amplitude of the stator current cannot exceed a specified maximum, (2) the amplitude of the stator flux cannot exceed a specified maximum, and (3) the stator voltage cannot exceed rated. If condition (2) is satisfied, then condition (3) is automatically satisfied for rotor speeds less than rated. Conditions (1) and (2) place limits on the slip frequency which may prevent operation in any of the modes described in the previous section. To establish these limits, it is useful to express the stator current and flux in terms of the selected independent variables. After extensive algebraic manipulation.

$$|\psi_s| = \sqrt{T_e} \sqrt{\frac{b}{\omega_s} + c\omega_s} < |\psi_s|_{max} \tag{28}$$

where

$$b = \frac{\omega_b r_r [X_m^4 + (X'')^2 X_{rr}^2 + 2X_m^2 X'' X_{rr}]}{X_{rr}^2 X_m^2} \tag{29}$$

$$c = ((X'')^2 X_{rr}^2)/(\omega_b r_r X_m^2) \tag{30}$$

$$|i_s| = \sqrt{T_e} \frac{\sqrt{X_{rr}}}{X_m} \sqrt{\left(\frac{1}{\tau_r \omega_s} + \tau_r \omega_s\right)} < |i_s|_{max} \tag{31}$$

Equations (28) and (31) establish limits on the slip frequency that can be set.

V. NUMERICAL EXAMPLE

It is instructive to illustrate the previous relationships for a specific machine. The machine selected is a 5-Hp cage rotor machine. The pertinent parameters are $r_s = 0.028$, $r_r = 0.014$, $X_M = 1.6271$, $X_{ls} = 0.1755$, $X_{lr} = 0.0879$. All data are in per unit with $Z_b = 14.182 \ \Omega$, $P_b = 3730 \ W$, $V_b = 132.8 \ V$, and $I_b = 9.363 \ A$.

Although it was assumed that there are three independent variables (torque, speed and slip frequency), it is seen in (24) that the efficiency is independent of torque. Thus, it is possible to plot the efficiency versus the remaining independent variables as shown in Fig. 2. Maximum efficiency occurs at a slip frequency of 2.55 rad/sec as calculated using (25) while MTA operation occurs at a slip frequency of 3.07 rad/sec as determined by (23). As shown in Fig. 2, there is little difference in the efficiency for these two operating modes.

In the FO control strategy, the slip frequency is a function of the commanded torque. The efficiency may be plotted versus torque and speed as shown in Fig. 3. As shown, the efficiency decreases substantially when either the torque or speed is small and is equal to zero when the torque and/or speed is zero.

The power factor is plotted as a function of slip frequency
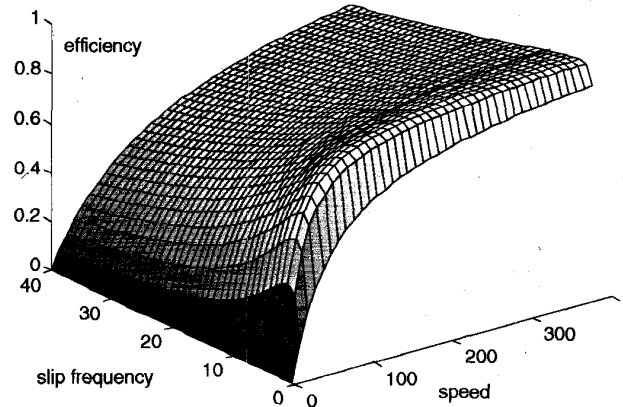

Fig. 2 Efficiency versus slip frequency and speed.
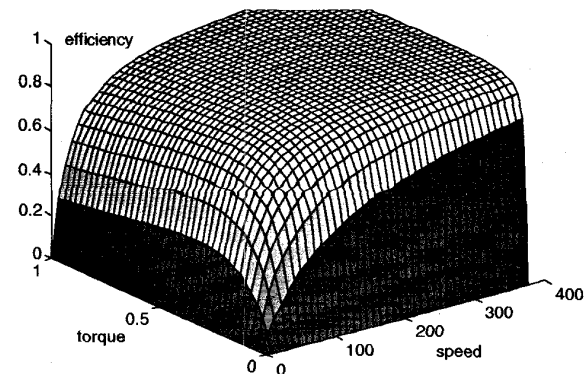

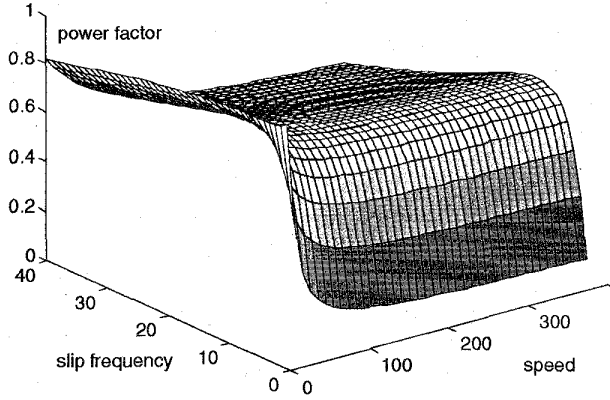Fig. 3 Efficiency versus torque and speed for FO control strategy.

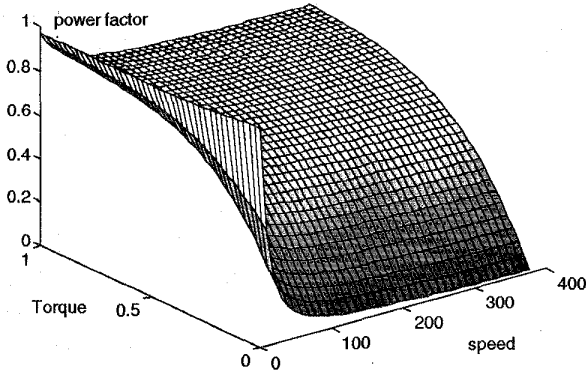Fig. 4 Power factor versus slip frequency and speed.

Fig. 5 Power factor versus torque and speed for FO control strategy.

Fig. 6 Stator flux amplitude versus torque and slip frequency.

Fig. 7 Stator current amplitude versus torque and slip frequency.

and speed in Fig. 4. In either ME or MTA modes, the power factor is significantly less than the maximum power factor which occurs at a slip of approximately 7 rad/sec. From Fig. 2, the efficiency at maximum power factor is somewhat less than either MTA or ME modes. Thus, it appears that if efficiency is the primary concern, operation at maximum power factor is not desirable. The power factor in the FO strategy is plotted in Fig. 5. Therein, it is seen that, for rotor speeds greater than about 50 rad/ sec, the power factor approaches zero as the torque approaches zero and is independent of rotor speed.

Although it is not apparent from the information depicted in Fig. 2, operation in the MTA or ME modes is not achievable if the desired electromagnetic torque becomes too large. This can be seen by plotting the stator flux and current amplitudes versus torque and speed as defined by (28) and (31). These relationships are plotted in Figs. 6 and 7, respectively. At rated torque, the minimum slip frequency that can be set is approximately 7.5 rad/sec. For smaller values of slip frequency, the flux amplitude will exceed rated. The minimum allowable slip is a function of the desired torque. For example, if the desired torque is reduced to 0.5 pu, the minimum slip frequency becomes 4 rad/sec. Although operation at a slip frequency higher than the minimum is possible, it is not desirable since, from Fig. 7, the stator current amplitude increases as the slip frequency is increased. This suggests that for large torques, the slip frequency should be set to the smallest value possible which does not violate the flux constraint. On the other hand, for smaller values of torque, the slip frequency should be set to the value given by (23). The global maximum torque per ampere controller which accomplishes these functions is described in the following section
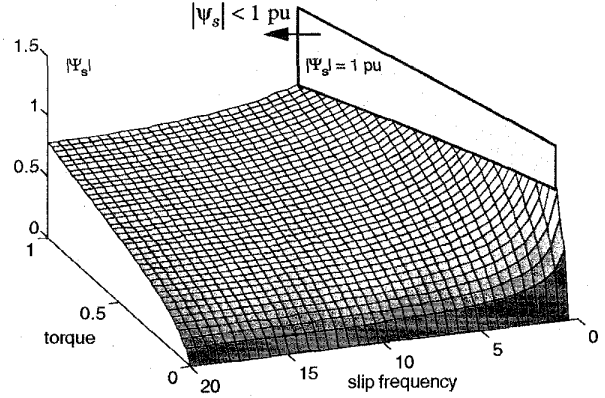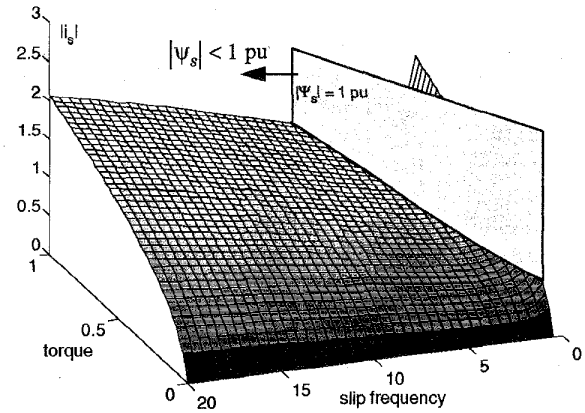
VI. GLOBAL MAXIMUM TORQUE PER AMPERE CONTROLLER

As long as the flux amplitude is less than rated, the optimum slip frequency is equal to the inverse rotor time constant. For larger values of torque, the slip frequency must be set to the smallest value possible which does not violate the flux constraint. An expression for the slip frequency in the flux-limited mode of operation may be established by setting $\left|\psi_s\right|$ to 1 in (28) and solving for ω_s. This gives

$$\omega_s = \frac{1 - \sqrt{1 - 4(T_e)^2 d}}{2 T_e c} \tag{32}$$

where

$$d = \frac{(X'')^2 [X_m^4 + (X'')^2 X_{rr}^2 + 2 X_m^2 X'' X_{rr}]}{X_m^4} \tag{33}$$

and c is given by (30). The breakpoint between the constant slip and flux-limited regions of operation may be established by setting ω_s in (32) to the optimal slip defined by (23) and solving for T_e. This sequence of operations yields

$$T_{e,bp} = \frac{\omega_b r_r X_{rr}}{b X_{rr}^2 + (c \omega_b r_r)^2} \tag{34}$$

A plot of ω_s versus T_e for the given machine is shown in Fig. 8. If the desired torque is less than $T_{e,bp} = 0.465$ pu, the slip frequency is set to the inverse rotor time constant. If the desired

torque is greater than the breakpoint value, the slip frequency is increased so as to maintain constant flux. As shown, the slip frequency is essentially a linear function of the desired torque in the flux-limited region. In this region, the stator current is minimized subject to the flux constraint.
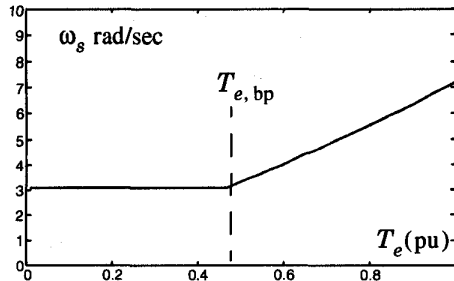

Fig. 8   Slip frequency versus torque for maximum torque per ampere subject to 1-pu flux constraint.

An expression for the stator current amplitude can be established from (31). For $T_e < T_{e,bp}$, the desired slip is given by (23) whereupon $\tau_r \omega_s = 1$. If $T_e > T_{e,bp}$, the desired slip is given by (32) whereupon

$$\tau_r \omega_s = \frac{[1 - \sqrt{1 - 4T_e^2 c}]X_m^2}{2T_e(X'')^2 X_{rr}} \tag{35}$$

In either case, $|i_s|$ is not a function of the rotor resistance since r_r cancels in the product $\tau_r \omega_s$.

An overall block diagram of the global maximum torque per ampere controller is shown in Fig. 9. Therein, T_e^* is the desired or commanded torque $|i_s^*|$ is the commanded current amplitude. The subscript "o" is used to distinguish the estimated machine parameters from the actual parameters which do not include this subscript. If the parameter estimates are equal to the actual machine parameters, this controller will result in operation at minimum stator current and close to maximum motor efficiency for all torques and speeds subject to the 1-pu flux constraint. The sensitivity of the controller to uncertainties in parameters is addressed in a later section. In any case, the proposed controller is designed so as to avoid operation under saturated conditions for all speeds and torques less than the corresponding rated values.
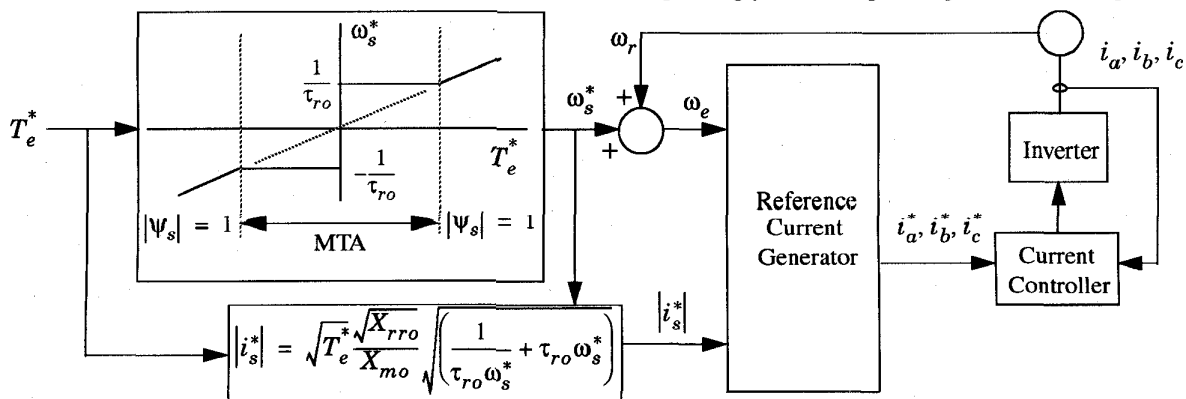
The efficiency and power factor of the selected machine are plotted in Figs. 10 and 11, respectively, using the global maximum torque per ampere (GMTA) controller. Comparing with Figs. 3 and 5 shows that, at a given speed, the efficiency remains essentially constant even for small values of torque. Moreover, the power factor is significantly higher at small values of torque. The latter characteristic is desirable since the converter losses are also likely to be reduced using the GMTA controller.

VII. SENSITIVITY TO PARAMETER VARIATIONS

It is well known that uncertainties in machine parameters, in particular the rotor resistance, can have adverse effects upon the performance of field-oriented drives [2]. It is useful, therefore to examine the effects of uncertainties in the rotor resistance on the MTA control set forth in the previous section. It is assumed here that all parameters are known exactly with the exception of rotor resistance. The rotor resistance given in Section V is assumed to be the estimated resistance which is held constant while the actual rotor resistance is varied. The resulting efficiency and flux amplitude are compared with the ideal controller in Figs. 12 and 13. As shown in Fig. 12, if the torque is less than approximately 0.5 pu, the efficiency is insensitive to rotor resistance variations. In the flux-limited region, if the actual resistance is somewhat smaller than the estimated resistance, the resulting flux amplitude will be somewhat smaller than rated and the efficiency will be reduced. On the other hand, if the actual resistance is larger than the estimated resistance, the efficiency is somewhat larger in the flux-limited region; however, the flux exceeds rated. If the magnetic circuit permits operation at this higher flux, this mode of operation may be desirable since the efficiency is higher; however, if saturation occurs, the efficiency plotted in Fig. 13 would likely be optimistic. A more thorough examination of the effects of magnetic saturation is currently underway.

VIII. CORE LOSS EFFECTS

Although core loss effects have been neglected in preceding analyses, they may have a significant effect on the overall efficiency [5]. During normal operating conditions, the rotor slip frequency is small; therefore, it is reasonable to assume that the rotor core losses will be negligible relative to the stator core losses [8]. Also, the stator core losses will be monotonically increasing functions of flux amplitude and stator frequency. For normal operation, the stator frequency will be close to the speed of the machine which is assumed to be given. Thus, it appears that core losses may be reduced by reducing the stator flux and, correspondingly, increasing the slip to maintain torque. However,
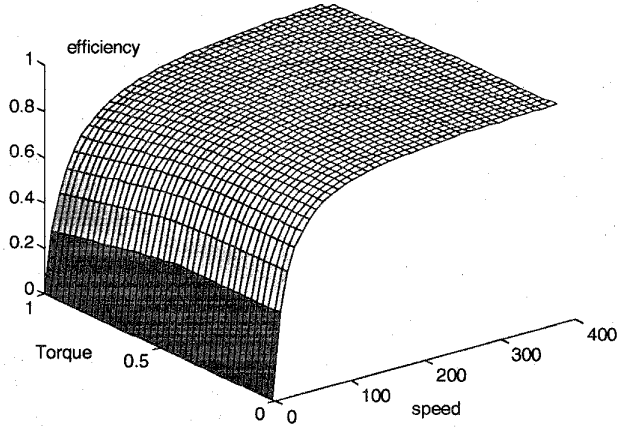

Fig. 9 Global maximum torque per ampere (GMTA) controller.

Fig. 10 Efficiency versus torque and speed using GMTA controller.

Fig. 11 Power factor versus torque and speed using GMTA controller.

Fig. 12 Efficiency versus torque as rotor resistance is varied.

Fig. 13 Stator flux versus torque as rotor resistance is varied.

this causes the stator current amplitude to increase causing the resistive (and inverter) losses to increase. If the reduction in core losses exceeds the increase in resistive losses, the motor efficiency will increase. Clearly, the optimum slip may be found using on-line search techniques. However, the hunting phenomenon observed in [8] suggests the improvement in overall efficiency may be insignificant relative to the simple GMTA strategy presented herein. Nonetheless, a more detailed evaluation of the overall system efficiency, which includes the effects of magnetic nonlinearities, core losses, and inverter losses, is presently under-way. It is important to note that the flux level in the proposed controller is less than or, for torques greater than the breakpoint defined by (34), essentially equal to the peak flux that would exist in FO or the well-known constant-volts-per-hertz strategies. Thus the core losses in the proposed controller will be less than or, at most, equal to the core losses in these existing strategies, regardless of rotor speed.

IX. DYNAMIC RESPONSE

In order to illustrate the dynamic characteristics of the GMTA controller, the drive system was simulated using ACSL [10]. The simulation was in detail with the switching characteristics of the inverter represented. It is assumed that the motor is initially deenergized and $\omega_r = 0$. The load torque is assumed to be proportional to the square of the rotor speed with rated torque produced at rated speed. The inertial time constant is $H = 0.5$ sec. It is assumed that the commanded torque is stepped to rated at $t = 0$. The resulting response is shown in
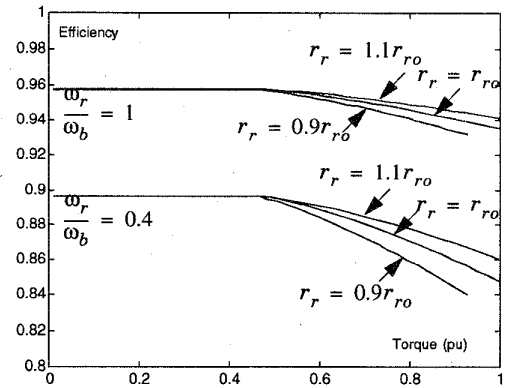
Fig. 14. For comparison purposes, the rotor speed response for a conventional FO controller is also plotted. When calculating the FO response, it is assumed that the initial rotor flux is equal to rated which gives rise to a near instantaneous step change in electromagnetic torque from zero to rated at $t = 0$. In the GMTA controller, the torque response is somewhat underdamped. It can be shown that the corresponding time constant is equal to the electrical time constant of the rotor. Although the FO response is somewhat faster, the overall time to reach rated speed is not significantly different.
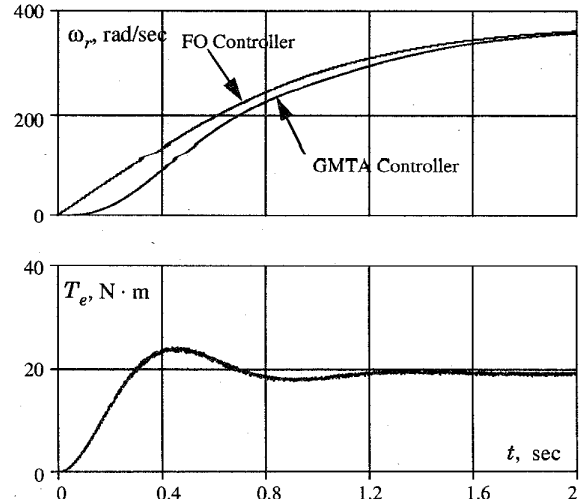

Fig. 14 Start-up response.

X. EXPERIMENTAL VERIFICATION

The given control strategy was implemented at the Electric Machines Laboratory at the University of Missouri-Rolla. The load torque was measured using an in-line torque sensor and the stator currents were measured using hall-effect current probes. A plot of the measured torque versus commanded torque is shown in Fig. 15 and a plot of the stator current amplitude is plotted in Fig. 16. Therein, measured data points are marked with an "+" and the solid lines represent predicted data. As shown, the measured and predicted data are in excellent agreement.
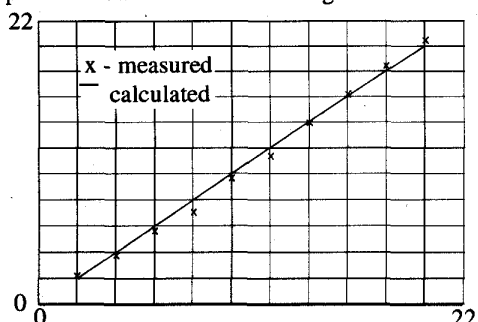
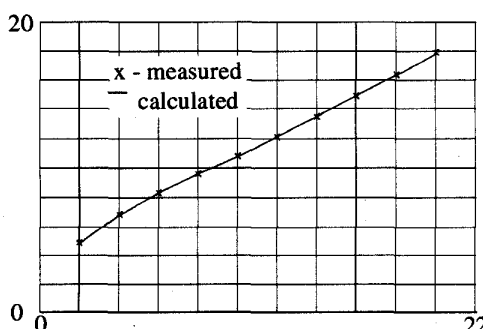

Fig. 15 Comparison of measured versus commanded torque.

Fig. 16 Comparison of calculated and measured stator current amplitude versus torque.

XI. CONCLUSIONS

A new control strategy for induction motor drives is presented which has the straightforward goal of minimizing the stator current amplitude for a given torque and speed. The controller is simple in structure and is relatively insensitive to rotor resistance variations. Although the torque response is not as fast as in field-oriented strategies, if the mechanical time constant is large relative to the rotor electrical time constant, the sacrifice in dynamic performance is insignificant. The performance of this controller has been illustrated for a 5-Hp squirrel cage motor. The proposed controller was also investigated for a high-speed 40-Hp motor being developed for aerospace applications and for a conventional 4-Pole 50-Hp 60-Hz motor. In each case, similar results were obtained.

XII. REFERENCES

[1] B. K. Bose, **Power Electronics and AC Drives**, Prentice-Hall, Englewood Cliffs, New Jersey, 1986.

[2] K. B. Nordin, D. W. Novotny, and D. S. Zinger, "The Influence of Rotor Parameters Deviations in Feedforward Field Orientation Drive Systems," *IEEE Transactions on Industry Applications*, Vol. IA-21, No. 4, July/August 1985.

[3] D. S. Kirschen, D. W. Novotny, and W. Suwanwisoot, "Minimizing Induction Motor Losses by Excitation Control in Variable frequency Drives," *IEEE Transactions on Industry Applications*, Vol. IA-20, No. 5, September/October 1984, pp. 1244-1251.

[4] H. G. Kim, S. K. Sul, and M. H. Park, "Optimal Efficiency Drive of a Current Source Inverter Fed Induction Motor by Flux Control," *IEEE Transactions on Industry Applications*, Vol. IA-20, No. 6, November/December 1984, pp. 1453-1459.

[5] S. K. Sul and M. H. Park, "A Novel Technique for Optimal Efficiency Control of a Current-Source Inverter-Fed Induction Motor, *IEEE Transactions on Power Electronics*, Vol. 3, No. 2, April 1988, pp. 192-198.

[6] P. Famouri and J. J. Cathey, "Loss Minimization Control of an Induction Motor Drive," *IEEE Transactions on Industry Applications*, Vol. 27, No. 1, January/February 1991, pp. 32-37.

[7] J. C. Moreira, T. A. Lipo, and V. Blasko, "Simple Efficiency Maximizer for an Adjustable Frequency Induction Motor Drive," *IEEE Transactions on Industry Applications*, Vol. 27, No. 5, September/October 1991, pp. 940-945.

[8] I. Kioskeridis and N. Margaris, "Loss Minimization in Scalar Controlled Induction Motor Drives with Search Controllers," *IEEE Transactions on Power Electronics*, Vol. 11, No. 2, March 1996, pp. 213-219.

[9] P. C. Krause, O. Wasynczuk, and S. D. Sudhoff, **Analysis of Electric Machinery**, IEEE Press, 1994.

[10] MGA Inc., **ACSL Reference Manual**, Edition 10, Concord, MA, 1991.

Oleg Wasynczuk (M' 76, SM'88) was born in Chicago, Illinois on June 26, 1954. He received the B.S.E.E. degree from Bradley University in 1976 an the M.S. and Ph.D. degrees from Purdue University in 1977 and 1979, respectively. Since 1979, he has been at Purdue where he is presently a Professor of Electrical and Computer Engineering. He is also a consultant for P. C. Krause and Associates. Dr. Wasynczuk is a member of Eta Kappa Nu, Tau Beta Pi and Phi Kappa Phi and is a Senior member of the IEEE Power Engineering Society.

Scott D. Sudhoff received the BSEE, MSEE, and Ph.D. degrees at Purdue University in 1988, 1989, and 1991, respectively. He is currently an Assistant Professor at the University of Missouri - Rolla. He is also a consultant for P. C. Krause and Associates. His interests include electric machines, electric drive systems, power electronics, flexible ac transmission, and finite-inertia power systems. He has authored or co-authored over 20 papers in these areas.

Keith A. Corzine received the BSEE and MSEE degrees from the University of Missouri-Rolla in 1992 and 1994, respectively, and is currently pursuing the Ph.D. degree. His interests include the design and analysis of electric machinery and electric drive systems. He has authored or co-authored 5 transaction papers in these areas.

Jerry L. Tichenor received the BSEE and MSEE degrees from the University of Missouri-Rolla in 1994 and 1996, respectively, and is currently an Associate Research Engineer at the University of Missouri-Rolla. His interests include electric drive systems and power electronics.

Irving G. Hansen was born in Toledo, Ohio in 1932. He received a BSEE from Tri-State University in 1957, and a MSEE from the University of Toledo in 1978. Until 1995, he was a senior electrical engineer at the NASA Lewis Research Center working in advanced technology for aerospace power systems. He holds two patents in aerospace instrumentation, and has published 28 articles on power electronics, components, and instrumentation. He is presently a technical consultant on electronic components and power systems.

Linda M. Taylor received her BEEE from the Youngstown State University in 1988 and has since been working as an electrical Engineer at the NASA Lewis Research Center. Her responsibilities involve developing advanced power systems and motor drives for aerospace applications and has authored or coauthored 5 papers in these areas.